Isı Bilimi ve Tekniği Dergisi, 31, 1, 27-36, 2011
J. of Thermal Science and Technology

ISSN 1300-3615

# EXPERIMENTAL MEASUREMENTS AND COMPUTATIONAL MODELING FOR THE SPRAY COOLING OF A STEEL PLATE NEAR THE LEIDENFROST TEMPERATURE

**Cemil YİĞİT*, Nedim SÖZBİR*, S. C. YAO** Hasan Rıza GÜVEN*** and Roy J. ISSA******
* Department of Mechanical Engineering, Sakarya University
54187 Esentepe, Sakarya, Turkey, cyigit@sakarya.edu.tr, sozbir@sakayra.edu.tr
** Department of Mechanical Engineering, Carnegie Mellon University
Pittsburgh, Pennsylvania,15213,USA, scyao@cmu.edu
*** Department of Mechanical Engineering, Istanbul University
34320 Avcılar, İstanbul, hrguven@istanbul.edu.tr
**** Department of Engineering and Computer Science, West Texas A&M University
TX-79016 Canyon, USA, rissa@mail.wtamu.edu

(Geliş Tarihi: 14. 05. 2009, Kabul Tarihi: 14. 04. 2010)

**Abstract:** Experimental studies and numerical simulations were conducted to reveal the heat transfer mechanism of impacting water mist on metal surfaces heated temperatures ranging from nucleate to film boiling regime. The test conditions of water mist cover the variations of air velocity from 0 to 50 m/sec, liquid mass flux from 0 to 7.67 $kg/m^2sec$, and surface temperature of stainless steel between $525^oC$ and $500^oC$. Local heat transfer coefficient and radial heat transfer distributions were measured at different air velocities and liquid mass fluxes. Experimental studies and computer simulations show that heat transfer coefficient increases not only with the air velocity but also with the liquid mass flux at the stagnation point. In addition, a small amount of water added in the impacting air jet, the heat transfer is significantly increased. For dilute spray, the mist heat transfer coefficient increases almost linear with the water mass flux. Results of computational study were compared against experimental data at atmospheric conditions, and the numerical model showed good accordance with the test data.
**Keywords:** Spray cooling, Experimental and Computational Spray Investigation.

# LEIDENFROST SICAKLIĞINDAKİ BİR ÇELİK PLAKANIN SPREY İLE SOĞUTULMASININ DENEYSEL ÖLÇÜMÜ VE SAYISAL MODELLEMESİ

**Özet:** Çekirdek kaynama rejiminden film kaynama rejimine kadar ısıtılmış metal yüzeylere çarpan su sisinin ısı transferi mekanizmasını ortaya çıkarmak için deneysel ve sayısal çalışmalar yürütüldü. Deneysel koşulların simülasyonunu yapmak için bir sayısal model geliştirildi. Deneysel çalışmada su damlacıklarını taşıyan havanın hızı 0-50 m/s, sıvı kütle akısı 0-7.67 $kg/m^2s$ ve paslanmaz çelik yüzeyin sıcaklığı $500\text{-}525^0C$ aralığında değişmektedir. Çeşitli hava hızları ve sıvı kütle akıları için lokal ısı transfer katsayısı ve radyal ısı transfer dağılımı ölçüldü. Deneysel ve sayısal çalışmalar göstermiştir ki, durgunluk noktasındaki ısı transfer katsayısı sadece hava hızıyla değil sıvı kütle akısıyla da artmaktadır. Buna ilaveten, hava jeti içerisine küçük miktarda su eklendiğinde ısı transfer katsayısı dikkate değer bir biçimde artmaktadır. Sıvı spreyinde ısı transfer katsayısı sıvı kütle akısıyla birlikte yaklaşık lineer olarak artmaktadır. Sayısal çalışmanın sonuçları deneysel verilerle karşılaştırıldı ve sayısal model deneysel verilerle iyi bir uyum göstermektedir.
**Anahtar Kelimeler:** Spreyle soğutma, Deneysel ve sayısal sprey incelemesi.

## NOMENCLATURE

| | |
|---|---|
| A | Area [$m^2$] |
| C | Specific heat [kj/kgK] |
| D | Nozzle opening diameter [m] |
| g | Gravitational acceleration [$m/sec^2$] |
| G | Liquid mass flux [$kg/m^2sec$] |
| h | Heat transfer coefficient [$W/m^2K$] |
| $h_{fg}$ | Latent heat of vaporization [kj/kg] |
| $h_{mist}$ | Mist heat transfer coefficient [$W/m^2K$] |
| k | Conductivity [W/mK] |
| m | Mass [kg] |
| $\dot{m}$ | Mass flow rate [kg/sec] |
| t | Time [sec] |
| T | Temperature [K] |
| u | Velocity [m/sec] |
| $\varepsilon$ | Emissivity |
| $\mu$ | Dynamic viscosity [Pa sec] |
| $\nu$ | Kinematic viscosity [$m^2/sec$] |
| $\rho$ | Mass density [$kg/m^3$] |

| | |
|---|---|
| $\sigma$ | Stefan-Boltzman constant [W/m$^2$K$^4$] |
| I | Turbulent intensity[=0.16Re$_D$$^{-1/8}$] |
| Nu | Nusselt number [=hD/k] |
| Pr | Prandtl number [=C$_p\mu$/k] |
| Re | Reynolds number [=uD/$\nu$] |
| We | Weber number [=$\rho\nu^2$D/$\sigma$] |

**Subscripts**

| | |
|---|---|
| a | Air |
| d | Droplet |
| l | Water |
| LF | Leidenfrost |
| m | Mixture |
| p | Constant pressure |
| r | Radiation |
| s | Surrounding |
| w | Wall |
| 0 | Stagnation point |

**Superscripts**

| | |
|---|---|
| * | Dimensionless quantity |

## INTRODUCTION

Water mist sprays have been used extensively in many industrial application because of the heat transfer benefits it has shown over conventional forced air. These applications include thin strip casting, glass tempering, electronic cooling. Currently, several investigators have studied the water mist cooling and thermal management of electronic devices. (Sözbir et.al., 2003; Issa and Yao, 2005a; Issa and Yao, 2005b; Yao et. al., 1989; Yao et. al., 2001) studied the spray cooling process. Cooling by water mist provides relatively uniform heat transfer; hence, it provides a better control of the material temperature. Additionally, it has high water usage efficiency, because water mist contains smaller droplets than traditionally water sprays. Furthermore, both water and air flow rates can be individually controlled to provide a wide range of heat transfer variations. In other words, it features both high efficiency and great flexibility of heat removal. Due to these advantages, water mist is used preferably in the cooling of thin metal sheets, in glass tempering at temperatures beyond Leidenfrost point, and in electronic chip cooling. In other applications, the aim is avoid distortion, and to minimize the stresses induced during the quenching process (Pietzsch et. al., 2005). (Sözbir and Yao, 2004) investigated water mist cooling for glass tempering experimentally. In this study, very high air jet impingement velocity was applied during glass tempering. The heat transfer of multiple water mist jets on glass was studied. The injection of mist with air during cooling considerably reduces the consumption of compressed air which results in considerable saving of air. When using mist cooling, the energy requirements of the system are significantly lowered. (Roy J. Issa et al., 2008) studied experinmetal and numerical modeling for the air mist cooling of a heated cylinder. (Strotos et. al., 2008) modeled water droplets impinging normal onto a flat heated surface under at atmospheric conditions in their study. Authors reported that impact velocity has a remarkable influence in the cooling of the heated plate, due to increased heat transfer numbers and wetting area. (Gambaryan-Roisman et. al., 2007) developed an experimental method to investigate the dynamics of liquid film produced by spray impact onto a heated target. According to the authors, the effectiveness of the spray cooling depends on the liquid volumetric flow rate. Additionally, the pray cooling process depends on the gravity level for high liquid flow rates. (Xishi et.al., 2004) performed a serried of experiments to investigate the hot solid surface cooling with water mist under different conditions, such as different initial surface temperatures and mist characteristics. The results show that the mist droplet cooling efficiency is significantly influenced not only by the surface initial temperature, but also by the mist characteristics, especially because of its Weber number. (Fujimoto et. al., 2008) investigated the effect of surface temperature, impact inertia and the spacing between the two droplets on the deformation behavior of liquid. Their investigation shows that the height of crown is larger with wider spacing between two droplets and higher impact inertia. (Nacheva and Schmidt, 2008) performed a numerical study to investigated the influence of different spray and model parameters on the evaporation efficiency and the HTC. Authors reported that the evaporation efficiency and the HTC depend on the mass flux, the droplet diameter and velocity. Spray cooling process is investigated in a wide range of scientific study, and several researchers issue empirical, semi-empirical, or numerical models to define the process and to compute the corresponding heat transfer coefficient (HTC). A comparison of the HTC calculated by some empirical models is presented in Fig. 1 (Nacheva and Schmidt, 2008). (Sozbir et. al., 2010) performed multiphase spray cooling of steel plates near the leidenfrost temperature.

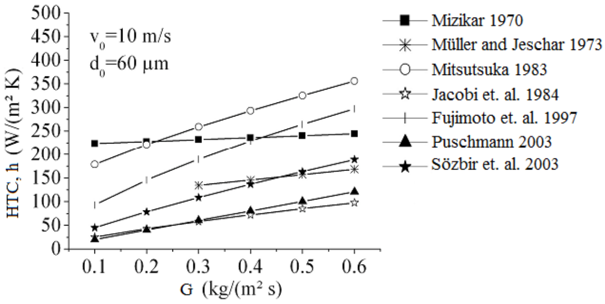


**Figure 1.** Comparison of HTC calculated with different correlations (Nacheva and Schmidt, 2008).

The objective of this study is to conduct experimental studies to reveal the heat transfer mechanism of impacting water mist on metal surfaces heated at temperatures ranging from nucleate to film boiling. In addition, a numerical model which based on the test setup conditions is developed to simulate water mist cooling process to support the interpretation of the experimental findings.

## EXPERIMENTAL STUDY

### Experimental Apparatus and Procedure

The experimental system is consisted of an air atomizer nozzle, an air flow system, a liquid supply system, an oven, a stainless steel test plate, and a data acquisition unit. A schematic diagram of the system is shown in Fig. 2. Overall experimental system setup is shown in Fig. 3. The air atomizer nozzle producing the mist flow is also depicted. A commercial air-atomizing nozzle (Spraying Systems Co., Air Atomizing, 1/8 J, Full Cone, Round Spray, and Spray Set-up No SU11), and an air chamber are used in this experiment. The chamber contains three air inlets and a pressure gauge. Upstream of the water line is an on-off solenoid valve. Downstream of the air chamber, has an exit opening 7.9 mm in diameter. Typically, the air atomizer nozzle produces a mist of 22.7 cm3/min (0.006 gpm) of water flow, about 20 micron volume median diameter, when applied with 96.5 kPa (10 psig) water pressure. The total spray angle is around 13 deg (Spraying Systems Co., Catalog 60).
The schematic of water mist jet impingement is shown in Fig. 4. Before the experiments were carried out, the local flow conditions were measured at a distance of 40 mm below the nozzle. This distance affects the air velocity and droplet mass flux. The approaching velocity of the impinging pure air was measured by TSI Air Velocity Meters (Velocicalc Model No. 8345/8346). The total air supply flow rate in the system was measured with a rotameter. The local liquid mass flux, G, was measured directly using a small cylindrical catcher. The total water supply flow rate in the system is measured with a rotameter.

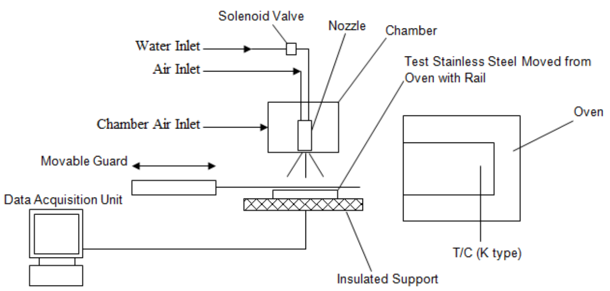


**Figure 2.** Schematic of experimental apparatus.

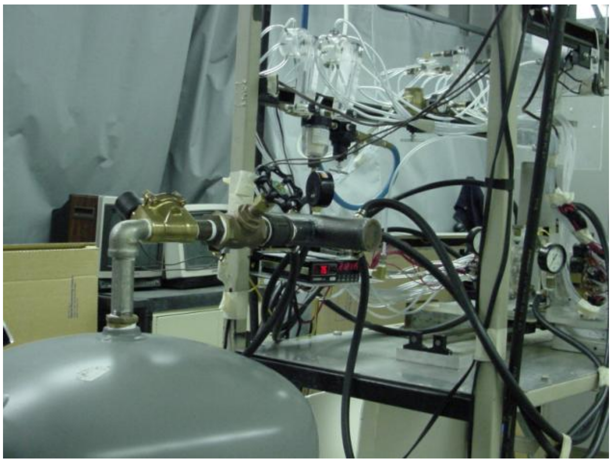

**Figure 3.** Overall experimental system setup.

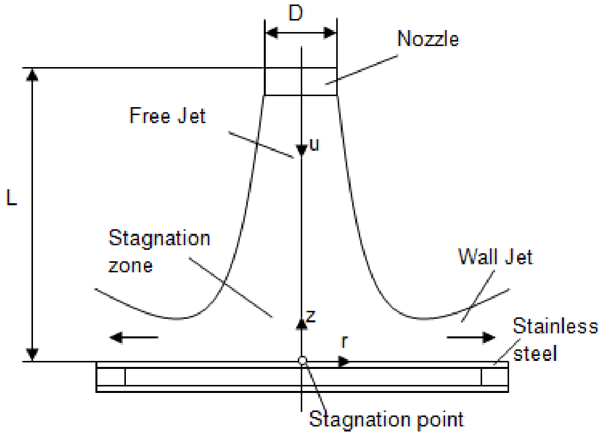


**Figure 4.** Schematic of water mist jet impingement onto surface.

The test plate is made of stainless steel (AISI304) with 101.6 mm in diameter, and 1 mm in thickness. Plates were regularly changed after a few tests. The nozzle is situated at a distance of 40 mm above and at the center of the plate. To measure the temperature-time history of test plate during cooling, two bare Type K thermocouple wires that are 0.1778 mm in diameter were attached to the backside of the plates by spot-welding. The wires were insulated using ceramic beads. Thermocouple locations are at the centerline and 2.54 mm offset from the centerline of the test plate's backside, as shown in Fig. 5. The backside of the plate was insulated with a shallow cavity. The temperature time histories were recorded using a digital data acquisition system (SP 2030, DAS 08/EXP 16).

At the beginning of the experiment, the test plate was heated to an initial temperature about 815-870$^{o}$C in the oven. The water mist from the nozzle was turned on, and the plate was taken out from the oven to put on the insulated cavity and underneath the shutter, which protects the plate from spray impingement. After the shutter was suddenly removed by the actuation of an air cylinder, the mist impinged on the heated surface.

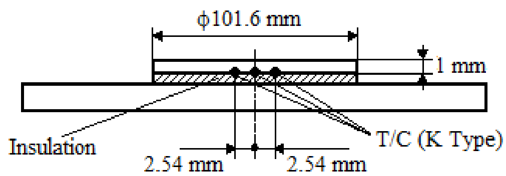


**Figure 5.** Test plate.

### Data Reduction

Throughout the test, the heated plate was positioned horizontally. It was found that the heat loss at the backside was mainly due to radiation. The temperature difference between the front side and the backside through the cooling transient was estimated to be within 10$^{o}$C. For a stainless steel plate of 1 mm thickness, the calculated Biot number based of the plate thickness ranged from 0.05 to 0.11. Therefore, it was reasonable to assume the lumped capacitance method to be valid in the evaluation of the surface heat flux. As a result, the inverse-conduction method was not necessary. The temperature measured at the backside of the plate was used to represent the mean temperature of the plate during the transient cooling.

Temperature recordings were collected at a sampling frequency of 50 data points per second. Only, the data between 525$^o$C to 500$^o$C (which were beyond the Leidenfrost temperature where droplets do not wet the surface) are used to evaluate the heat transfer at various conditions. In fact, this temperature range is also important to the glass tempering and steel rolling processes.

Since radial conduction is negligible over the thin plate, the lumped capacitance method can be applied to any specific region during cooling. The average heat transfer coefficient can then be calculated from:

$$mC_p(dT/dt) = hA(T_w - T_a) + \varepsilon\sigma 2A(T_w^4 - T_s^4) \qquad (1)$$

where $m$ is the disk mass, $C_p$ is the specific heat of the disk, $h$ is the convective heat transfer coefficient, $A$ is the disk heat transfer area at one side, $T_w$ is the disk surface temperature, $T_a$ is the air temperature, $T_s$ is the surrounding temperature (which is close to $T_a$), $\varepsilon$ is the emissivity, and $\sigma$ is the Stefan-Boltzman constant. The value of the emissivity used in the evaluation of the radiation heat transfer (from the front and backsides of the disk) is obtained from cooling tests where both air and water flows are turned off. Natural convective cooling heat transfer is evaluated and used in Eq. (1) to deduce the emissivity at this condition. Generally, radiative heat loss is on the order of 10-15 percent of the overall heat transfer during mist cooling in the percent study.

### Experimental Uncertainty

The measurement error of the air velocity is within 0.1 m/sec, the water mass flux is within 0.1 kg/m$^2$sec and the thermocouple reading is within 0.4 percent.

The thickness of stainless steel test plate is 1 mm, and the temperature difference between front side and backside during cooling is estimated to be within 10$^o$C. The cooling data, taken between 525$^o$C and 500$^o$C, are used to evaluate the change in temperature with time, *dT/dt*, as given in Eq. (1). Since this is well within the film-boiling regime, the rate of change in temperature is steady. Therefore, all the consistent errors, such as the assumption of lumped approach, will not affect *dT/dt* and the result of data reduction. This also reduces the possible error because the inversed conduction is not used. The estimated error of the deduced heat transfer coefficient is; therefore, in the order of 0.4 percent due to the uncertainty in the thermocouples readings.

Another possible source of error comes from the calibration of surface emissivity during the pure air-cooling tests. Considering a 5 percent error in the natural convection formula, the resulting error on the estimated emissivity will be on the order of 7 percent. When this emissivity is used in Eq. (1), an estimated error on heat transfer coefficient will be on the order of 0.85 percent. Combining this data reduction uncertainty with the thermocouple reading uncertainty, the overall uncertainty in the heat transfer coefficient is in the order of 1 percent.

## COMPUTATIONAL STUDY

Numerical computations are performed using FLUENT (6.3.26) software. An axisymmetric model which is used pressure based solver and implicit formulation is developed to simulate spray flow over a heated plate. The spray which is modeled DPM (Discrete phase model) consists of an air medium referred to as the continuous phase, and water droplets referred to as the discrete phase. The droplets are dispersed in the continuous phase and are traced stochastically in the Lagrangian reference frame. Fig. 6 shows the simulation of the spray mist in Fluent. Approximately a few thousand particle streams were injected to simulate the water mist spray. The trajectory of the droplet is solved by integrating the force balance on the droplet, where the inertial force is balanced by the drag force and the gravitational force. Drag coefficient between the droplet and air is calculated using the correlation given by (Morsi and Alexander, 1972).

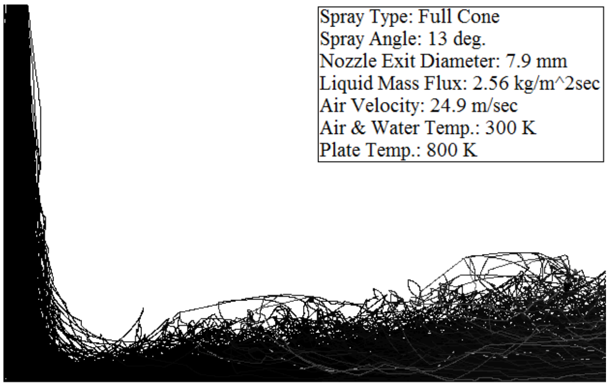


**Figure 6.** Water mist spray pattern at atmospheric conditions.

$$\frac{d\vec{u}_d}{dt} = F_D(\vec{u}_a - \vec{u}_d) + \frac{\vec{g}(\rho_d - \rho_a)}{\rho_d} + \vec{F} \qquad (2)$$

where F is droplet external force per unit mass and $F_D$ is drag force.

The droplet temperature is calculated from an energy balance on the droplet, where the sensible heat change in the droplet is balanced by the convective, radiative, and latent heat transfer between the droplet and gas-phase medium. Radiation heat transfer is calculated using the P-1 radiation model.

$$m_d c_{p,l}\frac{dT_d}{dt} = hA_d(T_s - T_d) + \frac{dm_d}{dt}h_{fg} + A_d\varepsilon_d\sigma\left(T_r^4 - T_d^4\right) \qquad (3)$$

Continuity, momentum, turbulence and energy equations are solved for water mist spray. The turbulence water mist flow model uses two equations in the k-ε method expressed in Eulerian coordinate. Intensity and length scale method is used for turbulent specification method. Turbulent intensity, I, can be represented as:

$$I = 0.16\,\mathrm{Re}_D^{-1/8} \tag{4}$$

The length scale for axisymmetric jet at various conditions is reported by (Versteeg and Malalasekera, 1995).

Weighing factors are used to concentrate the grid mesh near the plate surface and at the center of the computational domain. Hence, these domains are very important for computational accuracy. For water mist conditions a quadrilateral grid mesh of 160x140 provided acceptable numerical accuracy. The grid mesh of the model is shown in Fig. 7.

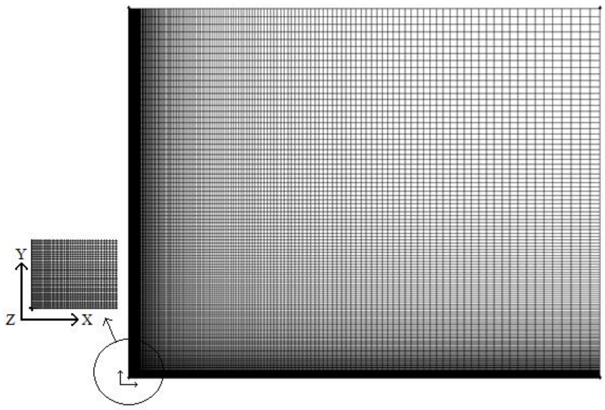


**Figure 7.** The mesh of the computational domain.

The physical properties of the liquid and gas phases were attained as function of the local temperature. Thermal conductivity of the mixture phase was obtained from a developed correlation in Eq. (5), which is modified to be accordant with experimental data to obtain the thermal conductivity of the mixture is developed by (Yiğit, 2009).

$$k_m = 2.9961^{0.0376 \cdot G^*} \cdot k_a\left(1+B\right) \tag{5}$$

where is $B$ constant and can be represented as:

$$B = 1-\left(\dot{m}_a/\dot{m}_l\right)\cdot\left(k_a/k_l\right) \tag{6}$$

The boundary conditions for the computational domain are shown in Fig. 8. The velocity inlet boundary, which is situated at the center of the plate at a distance of 40 mm above, is applied for the air. It is assumed that there is a small distance between injection plane and nozzle exit plane. Pressure outlet boundaries are applied to both horizontal edges except velocity inlet boundary and vertical edges of the computation domain. The wall boundary, is assumed to be at a fixed temperature, is applied to bottom of the computation domain.

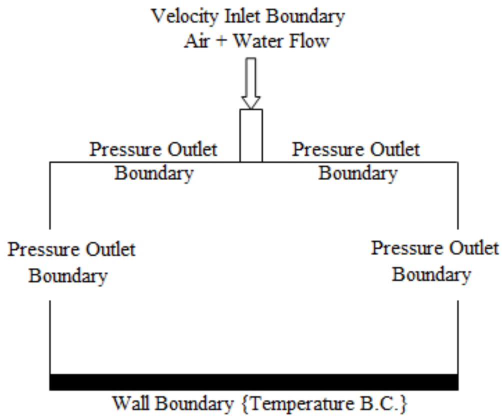


**Figure 8.** The model boundary conditions.

## RESULTS AND DISCUSSION

### Air Convection Cooling

The experimental results of air convective cooling without droplets are compared with numerical analysis at stagnation point in Fig. 9. Although the heat transfer of laminar round jet has been reported by (Incropera and Dewitt, 2001; Martin, 1977), the configuration of nozzle used in (Graham and Ramadhyani, 1996) is most relevant to the present study. They reported the three-dimensional stagnation point Nusselt number $Nu_{a,0}$ as:

$$Nu_{a,0} = \mathrm{Re}_D^{0.5}\,\mathrm{Pr}^{0.4} \tag{7}$$

Where the Reynolds number, $Re_D$, and stagnation point Nusselt number, $Nu_{a,0}$, are based on jet velocity and nozzle diameter then

$$Nu_{a,0} = h_{a,0} D/k_a \tag{8}$$

$$\mathrm{Re}_D = uD/\upsilon \tag{9}$$

where $u$ is the air velocity at the nozzle exit.

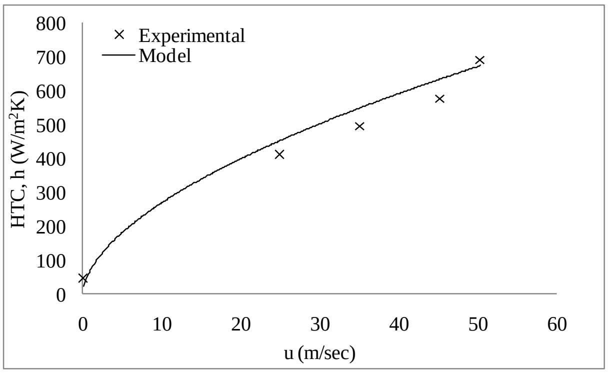


**Figure 9.** The comparison with experimental and numerical result of heat transfer coefficient at 500°C to 525°C, and 0 kg/m$^2$sec liquid mass flux.

Experimental and computational results are compared and demonstrated in Fig. 9. Experimental and computational errors range from 2.25% to 10.31%. The variation of heat transfer coefficient with air velocity is shown at the stagnation point. The experimental heat transfer data of pure air jet ($G$=0 kg/m$^2$sec) are compared to the summation of results from Eq. (7) and radiation heat transfer. The calculated $h$ is about 15 percent below the data. The discrepancy is likely due to the free stream turbulence that enhances the heat transfer of the jet (McCormick et. al., 1984). A similar observation has been addressed in (Deb and Yao, 1989) where a 15 percent free stream turbulence intensity induced 25 percent heat transfer enhancement. The reason for the present data showing a higher level for heat transfer is possibility due to the free stream turbulence in the air jet, which is induced by the complex internal geometry of the air passage in the nozzle. Considering this, the present data of pure air-cooling is compatible with the general expectation.

**Water Mist Cooling**

Experimental and computational results are compared and demonstrated in Fig. 10 which presents the variation of heat transfer coefficient for mist cooling with air velocity at various liquid mass fluxes, G. The data indicate that the heat transfer coefficient increases strongly with the liquid mass flux. When the air velocity increases, heat transfer coefficient also increases.

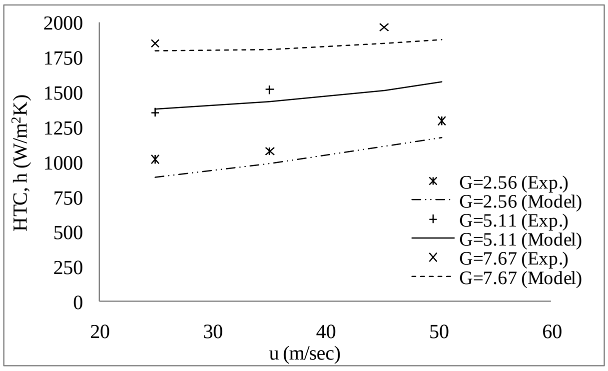


**Figure 10.** The comparison with experimental and numerical result of heat transfer coefficient at 500$^o$C to 525$^o$C, and liquid mass flux from 2.56 kg/m$^2$sec to 7.67 kg/m$^2$sec.

Since the liquid mass flux is the primary factor affecting the heat transfer coefficient, the heat transfer coefficient was replotted against the liquid mass flux in Fig. 11, where the connecting lines are best-fit curves of the data. Quantitatively, the heat transfer coefficients are improved dramatically with the presence of mist. For example, at 25 m/sec air velocity, a small liquid mass flux of 2.56 kg/m$^2$sec will only increase the heat transfer to more than double of air convection. It is also observed that the heat transfer coefficient is increased almost linearly with the liquid mass flux.

It is interesting to identify the respective effects of air jet and liquid mass flux on water mist cooling. The difference between the total heat transfer data and the pure air data, which is the summation of air jet convective heat transfer and the radiative heat transfer, is used to determine the heat transfer coefficient due to the cooling by water mist only. The water mist heat transfer coefficient can then be expressed as a function

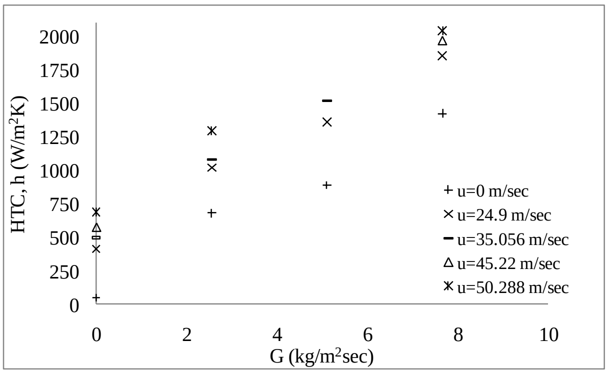


**Figure 11.** Experimental results for the heat transfer coefficient against the liquid mass flux.

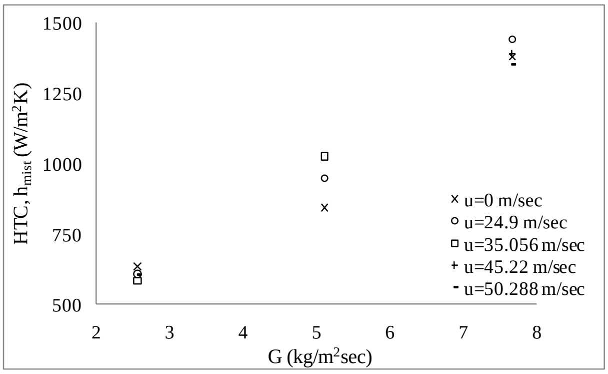


**Figure 12.** Experimental results for the difference of total and air heat transfer coefficient against the liquid mass flux.

of the liquid mass flux as shown in Fig. 12. The figure indicates that the heat transfer contribution of water increases monotonically with the water mass flux. When the mass flux increases, the effect is slightly less than linear. This is likely due to the interference effect between the droplets on the surface heat transfer. This occurs when the spray density increases and droplets are not having independent heat transfer because frequently the local surface temperature is not fully recovered before another droplet impact at the same point. Also the jet velocity does not influence significantly to the water mist heat transfer. In other words, droplet velocity has a relatively minor effect on the heat transfer of mist. This has also been reported earlier in (Deb and Yao 1989; Choi and Yao, 1987). The increase in velocity may increase the droplet deformation during surface impaction, but decrease the time duration of the interaction. These two effects tend to compensate each other when considering their effect on the heat transfer result. To correlate the primary of liquid mass flux, this water mist heat transfer coefficient can be represented as:

$$h_{mist} = 284G^{0.8} \tag{10}$$

When $h_{mist}$ is water mist heat transfer coefficient in W/m$^2$K and $G$ is liquid mass flux in kg/m$^2$sec. The relationship can be written in non-dimensional form as:

$$Nu_{mist} = 194\,\mathrm{Re}_l^{0.8} \tag{11}$$

where

$$Nu_{mist} = h_{mist} D/k_l \tag{12}$$

$$\mathrm{Re}_l = GD/\mu_l \tag{13}$$

It is noticed that the nozzle orifice diameter, $D$, is considered to be the characteristic length in order to be consistent with the air convection formulation.

Accordingly, the overall heat transfer of the dilute mist flow, without considering the radiation, can be predicted as the summation of air and water mist heat transfer coefficient components:

$$h_{conv} = h_{a,0} + h_{mist} \tag{14}$$

Where the $h_{a,0}$ can be evaluated from Eq. (7) and $h_{mist}$ from Eq. (11). Therefore, for water mist cooling at film boiling condition, the convective heat transfer of air and liquid mass flux can be accounted for separately.

**Radial Distributions**

The radial distribution of water mist heat transfer is important for the quality control during the cooling processes of metal and glass sheets. The radial water mass flux distribution of the spray was measured using several small tubes to catch the spray deposition directly. A typical result is shown in Fig. 13 at different flow rates. The resulting radial heat transfer distribution at different liquid mass fluxes is shown in Fig. 14. All the data are at a constant air velocity 35 m/sec. The locations of thermocouples are at center, 16.93 and 33.87 mm from the center stagnation point. In Fig. 14, the heat transfer coefficients at different radial locations are normalized by the heat transfer of mist flow at the stagnation point as described in Eq. (14). The figure indicates that the normalized redial heat transfer distribution of water is also very close to that of the pure air jet case. This is possibly due to the small size of water mist droplets (~20 μm). Since the droplets are entrained with the air, the deposition of the droplets and mist heat transfer distributions on the surface are similar to pure air flow case.

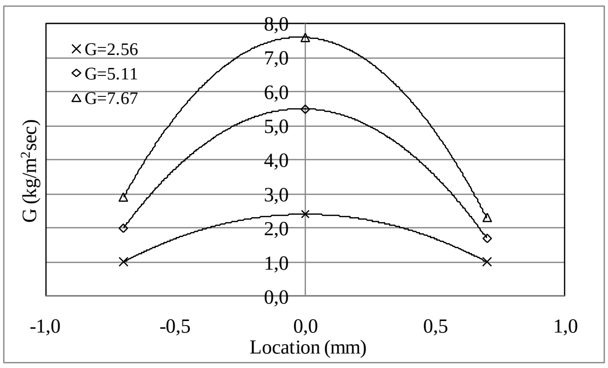


**Figure 13.** Experimental results for the radial spray liquid mass flux distributions (u=35 m/sec).

A comparison between the experimental and the computed heat transfer coefficients along the radial direction for the case where air velocity is 35 m/sec is shown in Fig. 15. Radial heat transfer distribution for various air velocities is obtained from computational analysis on stainless steel plate is shown Fig. 16. The highest heat transfer coefficient occurs at stagnation point which is the center of the plate. Therefore, the best cooling exists at the stagnation point and decreases further away from the plate center.

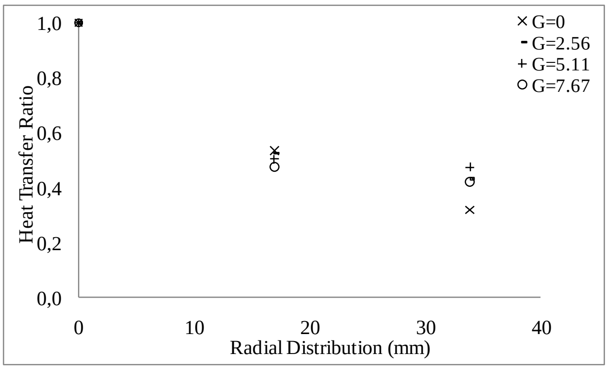


**Figure 14.** Experimental results for the heat transfer distributions on the radial direction of a single jet (u=35 m/sec).

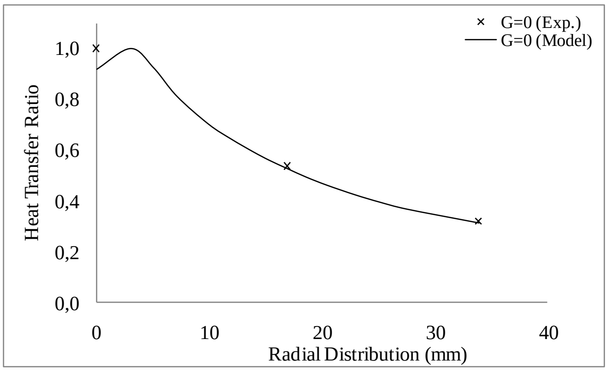


**Figure 15.** Experimental and computational heat transfer distribution on the radial direction for air velocity 35 m/sec.

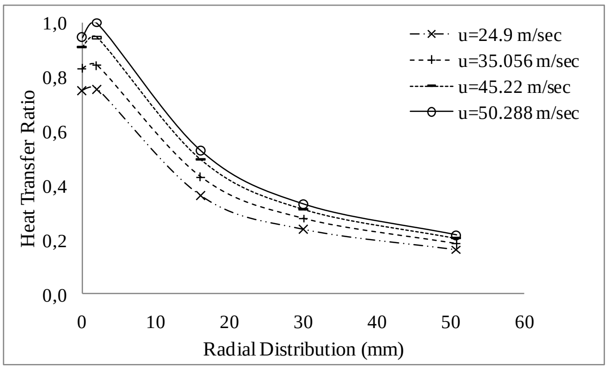


**Figure 16.** Radial heat transfer distributions on the plate obtained from numerical analysis at 2.56 kg/m$^2$sec liquid mass flux.

**Leidenfrost Temperature**

The experimental results for the Leidenfrost temperature, $T_{LF}$, at the center stagnation point of the plate are given with respect to the liquid mass flux, $G$, in Fig. 17. The Leidenfrost temperature is defined as the temperature associated with minimum heat flux on the film-boiling curve. Since the plate is only 1 mm thick and the cooling process takes only 2~3 seconds, the effect of radial conduction is negligible.

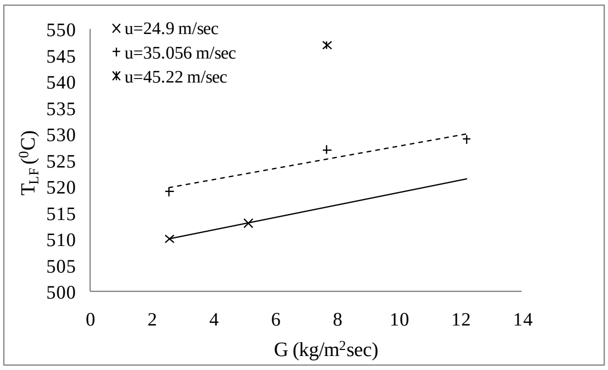


**Figure 17.** The variation of Leidenfrost temperature with liquid mass flux.

The data indicates that Leidenfrost temperature increases for larger values of liquid mass flux. These trends are similar to that reported by (Ishigai et. al., 1979; Hoogendoom and den Hond, 1974). However, the present experiment indicates that the Leidenfrost temperature also increases with increasing air velocity (for water mist cooling). At higher air velocity, the droplets impact on surface with more momentum, and induce the quenching easier. As a result, the Leidenfrost temperature is also higher.

## CONSLUSION AND RECOMENDATIONS

Experimental studies were conducted to reveal the heat transfer phenomena associated with dilute water mist sprays in the cooling of stainless steel plate heated temperatures ranging from nucleate to film boiling regime. A numerical model was also developed to simulate both the pure air and water mist cooling of high temperature metal surface at atmospheric pressure. Heat transfer coefficients were measured at various spray parameters such as air velocities and liquid mass fluxes. The variation of the Leidenfrost temperature with both the air velocity and the liquid mass flux was also discussed. The major conclusions of the study are:

1. With the injection of a small amount of water in the air jet, the heat transfer effectiveness dramatically increases. The water mist heat transfer coefficient increases with both the air velocity and the liquid mass flux. For dilute sprays, mist and air heat transfer are independent. Experimental and computational errors range from 2.99% to 12.53% for water mist spray cooling.
2. The convective air heat transfer is analyzed using a computational fluid dynamics model. Experimental and computational errors range from 2.25% to 10.31%.
3. For dilute sprays, the mist heat transfer coefficient increases almost linear with the water mass flux. The effect of air velocity is fairly small.
4. For dilute sprays, the overall convective heat transfer coefficient can be viewed as two separable components: heat transfer coefficient of air and liquid water which can be combined together to form the overall heat transfer coefficient. For general predictions, Eq. (11) suggests where Eq. (4) and Eq. (8) can be applied.
5. The radial distribution of heat transfer coefficients of water mist has a similar trend to air jet.
6. The best cooling exists at the stagnation point where the heat transfer coefficient is at its peak.
7. The Leidenfrost temperature increases with both the air velocity and the liquid mass flux.


## ACKNOWLEDGEMENT

This research is supported by Scientific Research Projects Committee of Sakarya University with project number 2006-FBD-002.


## REFERENCES


Choi, K. J., and Yao, S. C., Mechanism of Boiling Heat Transfer of Normally Impacting Spray, *Int. J. Heat Mass Transfer*, 30(2), 311-318, 1987.

Deb, S., and Yao, S. C., Analysis on Film Boiling Heat Transfer of Impinging Sprays, *Int. J. Heat Mass Transfer*, 32(11), 2099-2112, 1989.

Fujimoto, H., Hatta, N., Asakawa, H., and Hashimoto, T., Predictable Modeling of Heat Transfer Coefficient between Spraying Water and a Hot Surface above the Leidenfrost Temperature, *ISIJ Int.*, 37(5), 492-497, 1997.

Fujimoto, H., Tong, A. Y., and Takuda, H., Interaction Phoneme of Two Water Droplets Successively Impacting onto a Solid Surface, *International Journal of Thermal Sciences* 47(3), 229-236, 2008.

Gambaryan-Roisman, T., Kyriopoulos, O., Roisman, I., Stephan, P., and Tropea, C., Gravity Effect on Spray Impact and Spray Cooling, *Microgravity-Science and Technology* 19(3/4), 151-154, 2007.

Graham, K. M., and Ramadhyani, S., Experimental and Theoretical Studies of Mist Jet Impingement Cooling, *Journal of Heat Transfer* 118(2), 343-349, 1996.

Hoogendoom, C. J., and den Hond, R., Leidenfrost temperature and heat transfer coefficient for water spray impinging on a hot surface, *Proceeding of 5$^{th}$ International Heat Transfer Conference* 4, 135-138, 1974.

Incropera, F. P., and DeWitt, D. P., *Fundamentals of Heat and Mass Transfer*, John Wiley & Sons Inc., New York, 2001.

Industrial Spray Products, Spraying Systems Co. Catalog 60, Wheaton, IL.

Ishigai, S., Nakanishi, S., and Ochi, T., Mist Cooling of a Hot Surface, *Proceeding of the 16$^{th}$ National Heat Transfer Symposium of Japan* 316-321, 1979.

Issa, R. J., and Yao, S. C., A Numerical Model for The Mist Dynamics and Heat Transfer at Various Ambient Pressures, *Journal of Fluids Engineering-Transactions of the ASME* 127(4), 631-639, 2005a.

Issa, R. J., Hunt E.M. and Davis F.J., Experinetal Measurements and Numerical Modeling for the Air-Mist Cooling of A Heated Cylinder, *Proceedings of HT2008, ASME 2008 Summer Heat Transfer Conference,* August 10-14, 2008, Jacksonville, FL, USA.

Issa, R. J., and Yao, S. C., Numerical Model for Spray-Wall Impaction and Heat Transfer at Atmospheric Conditions, *Journal of Thermophysics and Heat Transfer* 19(4), 441-447, 2005b.

Jacobi, H., Keastle, G., and Wünnenburg, K., Heat Transfer in Cyclic Secondary Cooling during Solidification of Steel, *Ironmaking and Steelmaking* 11, 132-145, 1984.

Martin, H., Heat and Mass Transfer Between Impinging Jets and Solid Surfaces, *Adv. Heat Transfer* 13, 1-60, 1977.

McCormick, D. C., Test, F. L., and Lessman, R.C., (1984) The Effect of Free-Stream Turbulence on Heat Transfer from a Rectangular Prism, *ASME Journal of Heat Transfer* 106, pp. 268-275.

Mitsutsuka, M., Heat Transfer coefficients in the Surface Temperature range of 400 $^0$C to 800 $^0$C during Water-Spray Cooling of Hot Steel Product, *Tetsu-to-Hagane* 69, 268-274, 1983.

Mizikar, E.A., Spray Cooling Investigation for Continuous Casting of Billets and Blooms, *Iron and Steel Engineer* 53-60, 1970.

Morsi, S.A., and Alexander, A.J., An Investigation of Particle Trajectories in Two-Phase Flow Systems, *Journal of Fluid Mechanics* 55(2), 193-208, 1972.

Müller, H., and Jeschar, R., Untersuchung des Wärmeübergangs an einer simulierten Sekundärkühlzone beim Stranggießverfahren, *Eisenhüttenwesen,* (in German), 44, 589-594, 1973.

Nacheva, M., and Schmidt, J., Micro Model for the Analysis of Spray Cooling Heat Transfer-Influence of Droplet Parameters, *Micro-Macro-Interaction*, Springer Berlin Heidelberg, 159-172, 2008.

Pietzsch, R., Brzoza, M., Kaymak, Y., Specth, E., and Bertram, A., Minimizing of distortion of steel profiles by controlled cooling, *Steel Research Int.* 76, 399-407, 2005.

Puschmann, F., *Experimentelle Untersuchung der Sprühkühlung zur Qualitätsverbesserung durch definierte Einstellung des Wärmeübergangs*, PhD Thesis, (in German), University of Magdeburg, 2003.

Sözbir, N., Chang, Y. W., and Yao, S. C., Heat Transfer of Impacting Water Mist on High Temperature Metal Surfaces, *Journal of Heat Transfer* 125(1), 70-74, 2003.

Sözbir, N., and Yao, S. C., Experimental Investigation of Water Mist Cooling for Glass Tempering, *Atomization and Sprays* 14(3), 191-210, 2004.

Sözbir, N., Yiğit, C., Issa, R.J., Yao, S.C., Güven, H.R., and Özçelebi, S., Multiphase Spray cooling of Steel Plates near the Leidenfrost Temperature-Experimental Studies and Numerical Modeling, *Atomization and Sprays* 20(5), :387–405, 2010.

Strotos, G., Gavaises, M., Theodorakakos, A., and Bergeles, G., Numerical Investigation of The Cooling Effectiveness of a Droplet Impinging on a Heated Surface, *Int. J. Heat Mass Transfer* 51(19/20), 4728-4742, 2008.

Versteeg, H. K., and Malalasekera, W., *An Introduction to Computational Fluid Dynamics* (1$^{st}$ Ed.), Longman Group Ltd., England, 1995.

Yao, S. C., Impact Spray Boiling for Thermal Control of Electronic Systems, *ASME HTD-Heat Transfer in Electronics* 111, 129-133, 1989.

Yao, S. C., MEMS Enabled Micro Spray Cooling System for Thermal Control of Electronic Chips, *Proceeding of 2001 ASME International Mechanical Engineering Congress and Exposition,* IMECE, 2001.

Yiğit, C., (2009) *Numerical Studies of Using Spray Cooling on High Temperatures Surfaces*, PhD Thesis, (in Turkish), Mechanical Engineering Department, Sakarya University, Turkey, 2009.

Xishi, W., Guangxuan, L., Weicheng, F., and Dobashi, R., Experimental Study on Cooling a Hot Solid Surface with Water Mist, *Journal of Fire Science* 22(5), 355-366,2004.

**Cemil Yiğit**, 1977 yılında doğdu. 1999 yılında Sakarya Üniversitesi Makina Mühendisliği Bölümünü bitirdi. 2002 yılında Sakarya Üniversitesi Fen Bilimleri Enstitüsü Makina Mühendisliği EABD'dan Yüksek Lisans derecesi aldı. 2009 yılında yine aynı Üniversite'den doktora derecesi aldı.2001-2009 yılları arası Sakarya Üniversitesi Makine Müh. Bölümü'nde Ar.Gör., 2009 yılından itibaren Yrd. Doç. olarak görev yapmaktadır. Çalışma konuları sayısal ısı transferi, sprey ile soğutmadır.

**Nedim SÖZBİR**, 1986 yılında Yıldız Teknik Üniversitesi Kocaeli Müh. Fak. Mak. Müh bölümünde ve 1991 yılında da Fen Bilimleri Enstitüsü Makina Müh. EABD Yüksek Lisans yaptı. 1995 yılında İstanbul Üniversitesi Fen Bilimleri Enstitüsü Makina Müh. EABD doktora yaptı. 1994- Doktora tez çalışmasını1994-1995 yılları arasında Miami Üniveritesi Mak. Müh. Bölümünde yaptı. 1995 yılından itibaren Sakarya Üniversitesi Makina Mühendisliği Bölümününde Öğretim Üyesi olarak çalışmaktadır. 2000-2004 yılları arasında Carnegie Mellon Üniversitesi Mak. Müh. Bölümünde Misafir Öğretim Üyesi olarak görev yaptı. 2006-2007 yılları arasında Thales Alenia Space, Fransa firmasında Uydu Termal Kontrol konusunda çalıştı. 2006 yılında itibaren Ulaştırma Bakanlığı Türksat A.Ş' de Uydu Tasarım Danışmanı olarak görev yapmaktadır. Çalışma konuları, ısı transferi, ısıl sistemlerin tasarımı, sprey ile ısı transferi ve uydularda ısıl tasarımı ve kontrolüdür.

**Shi-Chune YAO**, Prof. Yao is a faculty member of the Mechanical Engineering Department at Carnegie Mellon University. Professor Yao's research interests are mainly at multiphase flow and heat transfer. This is closely related to energy and thermal control industries. He works on both experimental and theoretical researches on subjects which are important to industries but are fundamental in nature. Dr. Yao pioneered the spray cooling technology in 1989, and now the spray cooling is common on military electronics and in super-computers. Presently, our focus is on the evaporative micro-channel systems for the compact cooling devices. Due to the large surface to volume ratio, droplets and sprays are used broadly in many critical processes in industries. Professor Yao's research includes spray transport modeling, spray deposition, impaction coolings in metallurgical processes, micro-sprays for cooling of electronic chips, and drop combustion and flame propagation in fuel sprays. He has also conducted various numerical thermal modelings of material processes, which includes batch and continuous processes of sheet metals, and composite material thermal formings etc. Professor Yao is active in multiphase heat transfer research including fundamentals of boiling and heat transfer in tube bundles applied in energy industry. Currently he also works on micro-fluidics for micro-scale Direct Methanol Fuel Cell using the MEMS technology. This including the passive separation of gas bubbles from micro fuel cells, MEMS water management at cathode, and system designs.

**Hasan Rıza GÜVEN,** İstanbul Üniversitesi Makina Müh. Bölümde Öğretim Üyesi ve rektör danışmanı olarak görev yapmaktadır.

**Roy J. ISSA,** Dr. Issa is a faculty member of the Mechanical Engineering Department at West Texas A&M University. His background and research activities are in the area of heat transfer and fluid dynamics. He received his B.S. and M.S. degrees in Mechanical Engineering from University of Tennessee, Knoxville, and Ph.D. degree in Mechanical Engineering from University of Pittsburgh. Dr. Issa has worked for 4 years in the aerospace industry and 8 years in the steel industry. He has conducted extensive studies and on-line modeling on the cooling of the hot mill rolls and flat products on the run-out table. His current academic research activities focus on experimental studies of air-mist cooling in the metal production, power generation, food processing and meat industries